



Influencia de las condiciones de activación sobre la resistencia a la compresión, microestructura y productos de reacción de cementos de ceniza de bagazo de caña de azúcar

Influence of activation conditions on the compressive strength, microstructure, and reaction products of sugarcane bagasse ash cements

Lester Javier Espinoza Pérez*, Zugania Zelmira Zuniga García

Universidad Nacional de Ingeniería. Facultad de Ingeniería Química. Managua, Nicaragua.

*lester.espinoza@fiq.uni.edu.ni

(recibido/received: 15-febrero-202; aceptado/accepted: 06-junio-2022)

RESUMEN

Pastas de ceniza de bagazo de caña de azúcar (CBCA) y cemento de aluminato de calcio (CAC) fueron activadas con soluciones de silicato de sodio, variando el contenido de CBCA (80-95 % en peso), la relación $\text{SiO}_2/\text{Na}_2\text{O}$ (8-14 % en peso respecto al peso de CBCA), y la temperatura de curado (20 y 40 °C o 100 y 200 °C). Se obtuvieron resistencias a la compresión a los 28 días entre 5-20 MPa. Los resultados son cercanos a los reportados en la literatura para pastas de CBCA/metacaolin. En general, se observó que la resistencia a la compresión disminuyó con el aumento de la temperatura de curado de 100 a 200 °C. La ganancia en la resistencia a la compresión se atribuyó a la formación de una matriz densa de productos de reacción amorfa como C-S-H, N-A-S-H, C-A-S-H o gel de sílice. Nuestros resultados enfatizan la posibilidad de utilizar mayores contenidos de ceniza de bagazo de caña de azúcar para obtener cemento activado con álcali con resistencias a la compresión de hasta 20 MPa. Actualmente se está trabajando más para identificar el efecto de algunas variables en la resistencia a la compresión de los materiales compósitos.

Palabras claves: cemento activado con álcalis; ceniza de bagazo de caña de azúcar; cemento de aluminato de calcio; resistencia a compresión; microestructura; productos de reacción.

ABSTRACT

Pastes of sugarcane bagasse ash (SCBA) and calcium aluminate cement (CAC) were activated with sodium silicate solutions, varying the SCBA content (80-95 wt.%), the $\text{SiO}_2/\text{Na}_2\text{O}$ ratio (8-14 wt.% respect to the weight of SCBA), and the curing temperature (20 and 40 °C or 100 and 200 °C). 28 days-compressive strength between 5-20 MPa were obtained. The results are close to the reported in the literature for pastes of SCBA/metakaolin. Overall, it was observed that the compressive strength decreased with the increase in the curing temperature from 100 to 200 °C. The gain in the compressive strength was attributed to the formation of a dense matrix of amorphous reaction products such as C-S-H, N-A-S-H, C-A-S-H, or silica gel. Our results stress the feasibility to use higher contents of sugarcane bagasse ash to obtain alkali-activated cement with compressive strengths up to 20 MPa. Further work is currently underway to identify the effect of some variables on the compressive strength of composites.

Keywords: alkali-activated cement; sugarcane bagasse ash; calcium aluminate cement; compressive strength, microstructure, reaction products.

1. INTRODUCTION

Sugarcane bagasse ash (SCBA) is an abundant industrial waste of the sugar and ethanol industry, that generally can be used as a fertilizer, or disposed of in landfills (Xu et al., 2018), however, also can be used to produce alkali-activated cement (AAC) of less CO₂ emission than Portland cement (PC) which are of 0.65-0.92 kg CO₂/kg PC (Ali et al., 2011; Escalante García, 2002; Pour-Ghaz, 2013). It is important to notice that studies related to the use of SCBA as a precursor in the production of AAC are scarce (Payá et al., 2017).

Alternative cementitious materials and technologies are needed for structural and nonstructural applications; AAC based on precursors from urban and/or industrial wastes are a promising alternative. The most studied byproduct precursors are blast furnace slag (BFS), fly ash (FA), urban and industrial waste glass (WG), silica fume (SF), SCBA, rice husk ash, etc. SCBA has a chemical composition and amorphous structure that make it thermodynamically unstable and chemically reactive towards alkalis (NaOH, KOH, Na₂SiO₃, between others).

In some cases, the use of binary systems has been used to enhance the hydraulic and mechanical properties of the alkali-activated systems formed, for example, some authors have activated SiO₂-rich precursors in conjunction with sources of CaO to promote the formation of hydraulic reaction products such as C-S-H gel (C: CaO, S: SiO₂, H: H₂O). L.E. Menchaca-Ballinas and J.I. Escalante-Garcia (Menchaca-Ballinas & Escalante-Garcia, 2019) investigated binders of WG activated with CaO and NaOH; the CaO favored the dissolution of WG and provided Ca²⁺ for the formation of C-S-H, the specimens showed hydraulic behavior and increasing strengths of 15 and 29 MPa after 28 and 180 days, respectively. M. Vafaei and A. Allahverdi (Vafaei & Allahverdi, 2017) studied WG activated with sodium silicate solutions with different Na₂O contents, they incorporated up to 24% of three types of calcium aluminate cement (CAC); the optimized formulation mortar reached a compressive strength of 87 MPa with 10% Na₂O; the inclusion of CAC led to the formation of N-A-S-H gel (N: Na₂O, A: Al₂O₃, S: SiO₂, H: H₂O). C. Tippayasam and co-workers (Tippayasam et al., 2014) reported the use of 100% SCBA as a precursor for the production of AAC, obtaining 91 days-compressive strength of 5.68 MPa. However, when binary systems such as metakaolin/SCBA were used, higher compressive strengths were achieved as compared with 100% SCBA (16.80 MPa after 91 curing days). V.N. Castaldelli and co-workers (Vinicius N. Castaldelli et al., 2013) studied the activation of binary systems BFS/SCBA mortars with two different alkaline activators (NaOH and sodium silicate solutions) and obtained values about 60 MPa of compressive strength for BFS/SCBA systems after 270 days of curing at 20 °C; C-N-S-A-H gel (C: CaO, N: Na₂O, S: SiO₂, A: Al₂O₃, H: H₂O) was the main reaction product in all cases. V.N. Castaldelli and co-workers (V. N. Castaldelli et al., 2016) also studied the use of the binary system of FA/SCBA in the production of AAC using potassium silicate as the alkaline activating solution and found that the compressive strengths of mortars were influenced by the SiO₂/K₂O ratio and the FA/SCBA ratio, with values ranged 23–36 MPa after 7 days of curing at 65 °C and 28–40 MPa after 270 days of curing at 20 °C.

Although sodium silicate solution (also called waterglass) is effective to activate alternative materials, its production is expensive and environmentally difficult as it requires heating of sand as SiO₂ source and Na₂CO₃ at about 1000 °C, releasing 1.5 kg CO₂/kg sodium silicate (Turner & Collins, 2013). Recently, SCBA and other waste materials have been reported as a source of Si to produce waterglass employing different routes. H.K. Tchakouté and co-workers (Hervé Kouamo Tchakouté et al., 2017) used SCBA as a precursor to obtain sodium waterglass to activate metakaolin-based geopolymer cement and found that the

compressive strength of the resulting geopolymer cement cured at room temperature for 28 days was 32.9 MPa. Samples soaked for 28 days in water in parallel experiments revealed strength of 31.4 MPa. This shows that exposure to water does not lead to any weakening. Moreover, H.K. Tchakouté and co-workers (Hervé K. Tchakouté et al., 2016) used rice husk ash and WG to produce sodium waterglass to prepare metakaolin-based AAC; they concluded that waterglass from WG was more reactive and favored higher compressive strength of 40 MPa at 56 days.

In this work, we studied the effect of alkali concentration, $\text{SiO}_2/\text{Na}_2\text{O}$ ratio and curing temperature on the compressive strength, reaction products, and microstructures of pastes of the SCBA/CAC binary system. Our results stress the feasibility to use higher amounts of industrial wastes such as SCBA (in high SCBA content of 85-95 wt.%) to obtain AAC with compressive strength between 5-20 MPa, without the use of clinker. Probably, the main reaction products were the typical C-S-H, N-A-S-H, C-A-S-H gel (C: CaO, A: Al_2O_3 , S: SiO_2 , N: Na_2O , H: H_2O), possibly mixed with silica gel.

2. EXPERIMENTAL

2.1. Raw materials

Sugarcane bagasse ash (SCBA) from the Monte Rosa sugar mill, located in Chinandega city, Nicaragua, was used as SiO_2 source. Due to its humidity content, the SCBA was previously oven-dried at 90 °C for 24 h. Subsequently, it was ground for 5 minutes in an attrition mill, with a ball/powder ratio of 25/1. On the other hand, commercial calcium aluminate cement (CAC from POSSEHL) was used as CaO and Al_2O_3 source. The average particle size of both precursors was measured by laser diffraction (Coulter LS230), being 12.71 and 10.25 μm for SCBA and CAC, respectively. SCBA was substituted by 5, 10, and 15 wt.% of CAC in the composites.

Cementitious properties of SCBA were chemically activated with sodium silicate solutions with Na_2O concentration of 8, 10, 12 and 14 wt.% respect to the weight of SCBA. Also, the modulus of sodium silicate solutions ($\text{SiO}_2/\text{Na}_2\text{O}$ ratio) was modified at values of 0, 0.5, 1.0 and 1. using NaOH pellets of industrial grade.

2.2. Sample preparation

The cementitious composites SCBA/CAC were prepared by first homogenizing the dry precursors for 5 minutes in a blender with a planetary movement at low velocity and then was added the waterglass solution and homogenized for 10 minutes more. The pastes were cast in cylinder-shaped specimens (5cm per diameter and 1cm per high) using hydraulic pressing, applying a load of 330 kg/cm^3 per 1 minute; the cylinders were taken to set in an oven at 40 °C for 24 h, covered with plastic films to avoid water losses. The solidified specimens were demolded and continued curing in isothermal chambers at 20 or 40 °C until 28 days. Finally, the cylinder-shaped specimens were cut into cubes of 1cm per side to be characterized. Table 1 present the composition of pastes prepared.

Table 1. Composition of pastes prepared.

Nomenclature*	CAC (wt.%)	SCBA (wt.%)	Na_2O (wt.%)	$\text{SiO}_2/\text{Na}_2\text{O}$ ratio	Curing temperature (°C)
95-8-0	5	95	8	0	40(24h)-20(28 days)
95-10-0.5	5	95	10	0.5	40(24h)-20(28 days)
95-12-1	5	95	12	1	40(24h)-40(28 days)
95-14-1.5	5	95	14	1.5	40(24h)-40(28 days)

90-8-0.5	10	90	8	0.5	40(24h)-40(28 days)
90-10-0	10	90	10	0	40(24h)-40(28 days)
90-12-1.5	10	90	12	1.5	40(24h)-20(28 days)
90-14-1	10	90	14	1	40(24h)-20(28 days)
85-8-1	15	85	8	1	40(24h)-20(28 days)
85-10-1.5	15	85	10	1.5	40(24h)-20(28 days)
85-12-0	15	85	12	0	40(24h)-40(28 days)
85-14-0.5	15	85	14	0.5	40(24h)-40(28 days)
80-8-1.5	20	80	8	1.5	40(24h)-40(28 days)
80-10-1	20	80	10	1	40(24h)-40(28 days)
80-12-0.5	20	80	12	0.5	40(24h)-20(28 days)
80-14-0	20	80	14	0	40(24h)-20(28 days)

*Nomenclature: x - y - z , where x , y and z denote the wt.% of SCBA, wt.% of Na_2O and $\text{SiO}_2/\text{Na}_2\text{O}$ ratio used in each formulation, respectively.

Later, four formulations of Table 1 were selected based on statistical analysis. The selected samples were prepared following the procedure described above, but the cylinders were taken to set in an oven at 100 or 200 °C for 24 h, covered with plastic films to avoid water losses. Then, the solidified specimens were demolded and continued curing in isothermal chambers at 20 °C until 28 days. Finally, the cylinder-shaped specimens were cut into cubes of 1cm per side to be characterized. Table 2 present the composition of selected pastes:

Table 2. Composition of selected pastes.

Nomenclature	CAC (wt.%)	SCBA (wt.%)	Na_2O (wt.%)	$\text{SiO}_2/\text{Na}_2\text{O}$ ratio	Curing temperature (°C)
95-10-0.5	5	95	10	0.5	100(2h)-20(28 days)
90-10-0	10	90	10	0	or
90-14-1	10	90	14	1	200(2h)-20(28 days)
85-14-0.5	15	85	14	0.5	

2.3. Characterization techniques

The chemical composition of SCBA and CAC was determined by the X-ray Fluorescence technique (XRF- BRUKER S4 PIONNER), with a 4kW excitation source, the data interpretation was done using the SPECTRA plus software. The 28 days-compressive strength was measured using a hydraulic press applying a rate of 250 N/s; the data reported represent the average of 3 measurements. The mineralogy of selected pastes was qualitatively characterized by X-ray diffraction using a Phillips PW3040 X-ray Diffractometer, in a range of 10°-50° 2 θ using a step size of 0.03° and 3 s per step, with $\text{CuK}\alpha$ radiation of 1.542 Å wavelength. For the microstructural characterization, scanning electron microscopy (Phillips XL30ESEM) was used for selected pastes. The specimens were mounted in resin and abraded using SiC paper from 80 to 1200 and polished using diamond pastes down to 1/4 μm . Graphite coating was applied to make the samples conductive under the microscope operated at a high vacuum and accelerating voltage of 20 kV, a spot size of 4–5, and a working distance of 10 mm at 20keV; the SEM was equipped with energy-dispersive X-ray spectroscopy.

3. RESULTS AND DISCUSSION

3.1. Characterization of raw materials

Figure 1 presents the X-ray diffraction (XRD) pattern for SCBA used as raw material, showing a halo between 15- 33°2θ, characteristic of amorphous materials; also, it was identified the presence of two crystalline phases: albite (NaAlSi₃O₈) and anorthite (CaAl₂Si₂O₈). Due to its high amount of amorphous or partially crystalline silica, this SCBA can be used as a precursor to obtaining AAC (De Soares et al., 2016). Crystalline silica is generally associated with high incineration temperatures (> 800 °C) and long incineration times (Cordeiro et al., 2009; Morales et al., 2009).

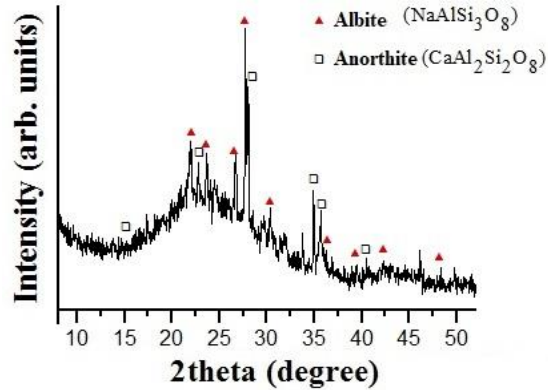


Figure 1. XRD pattern of SCBA used as raw material.

Figure 2 shows the microstructure of SCBA used as a raw material. It was observed the presence of particles with spherical, elongated, and irregular shapes and sizes ranged from 10-150 μm. Overall, almost all the particles showed the presence of porosity. It is important to note that said porosity can lead to an increase in the demand for water necessary to achieve good workability of the mixtures, which can cause a decrease in the compressive strength.

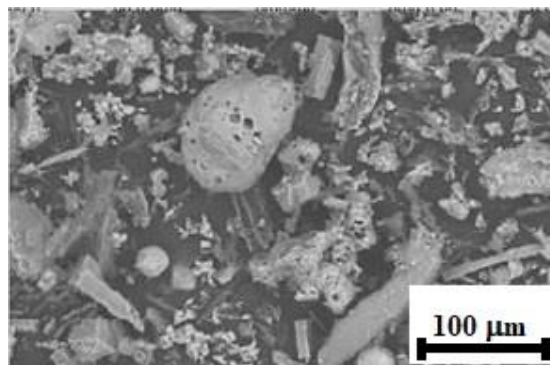


Figure 2. Morphology of SCBA used as raw material.

Furthermore, the chemical composition of both precursors is shown in Table 3:

Table 3. Chemical composition of both precursors.

Oxide (wt%)	CaO	SiO ₂	Al ₂ O ₃	MgO	SO ₃	TiO ₂	K ₂ O	Fe ₂ O ₃	Na ₂ O	P ₂ O ₅	LOI
SCBA	4.8	58.4	5.7	0.7	0.5	0.6	5.1	10.3	0.2	1.6	11.4
CAC	48.62	4.38	36.19	0.265	-	3.21	0.276	3.93	-	0.358	2.55

It can be seen from Table 3 that SCBA is a silica-rich material (~58 wt.% SiO₂), but the loss of ignition (LOI) of about 11 wt.% could be correlated with the presence of organic material and also can increase the water demand necessary to achieve good workability, thus, reducing the compressive strength (Bahurudeen & Santhanam, 2015). It is expected that a silica-rich material (just like SCBA or WG) induce the formation of silica gel as the main reaction product, nonetheless, it has been demonstrated that this type of reaction product lack of hydraulicity, the matrix is dissolved in water (Menchaca-Ballinas & Escalante-Garcia, 2019). As was mentioned above, it is common the use of precursors that provide a source of CaO or CaO-Al₂O₃ to induce the formation of hydraulic reaction products such as C-S-H, N-A-S-H or C-A-S-H gels. From Table 3, it can be deduced that calcium aluminate cement (CAC) was used as a source of CaO (~49 wt.%) and Al₂O₃ (~36 wt.%).

Finally, analysis by XRD (not shown in this work) showed that commercial CAC was formed by crystalline monocalcium aluminate (CaAl₂O₄) as the main component and minor amounts of crystalline phases such as Gehlenite Ca₂Al(AlSiO₇) and Mayenite (CaO)₁₂(Al₂O₃)₇.

3.2. 28-days compressive strength of SCBA-CAC composites

Table 4 shows the 28 days-compressive strength measured for all pastes from Table 1. As can be seen from Table 4, all the pastes had a very low mechanical performance, with 28-days compressive strengths between 0.10-0.65 MPa.

Table 4. 28 days-compressive strength for all pastes.

Nomenclature	CAC (wt.%)	SCBA (wt.%)	Na ₂ O (wt.%)	SiO ₂ /Na ₂ O ratio	Curing temperature (°C)	28 days-Compressive strength (MPa)
95-8-0	5	95	8	0	40(24h)-20(28 days)	0.48
95-10-0.5	5	95	10	0.5	40(24h)-20(28 days)	0.11
95-12-1	5	95	12	1	40(24h)-40(28 days)	0.23
95-14-1.5	5	95	14	1.5	40(24h)-40(28 days)	0.20
90-8-0.5	10	90	8	0.5	40(24h)-40(28 days)	0.14
90-10-0	10	90	10	0	40(24h)-40(28 days)	0.65
90-12-1.5	10	90	12	1.5	40(24h)-20(28 days)	0.37
90-14-1	10	90	14	1	40(24h)-20(28 days)	0.10
85-8-1	15	85	8	1	40(24h)-20(28 days)	0.13
85-10-1.5	15	85	10	1.5	40(24h)-20(28 days)	0.11
85-12-0	15	85	12	0	40(24h)-40(28 days)	0.36
85-14-0.5	15	85	14	0.5	40(24h)-40(28 days)	0.16
80-8-1.5	20	80	8	1.5	40(24h)-40(28 days)	0.19
80-10-1	20	80	10	1	40(24h)-40(28 days)	0.14
80-12-0.5	20	80	12	0.5	40(24h)-20(28 days)	0.28
80-14-0	20	80	14	0	40(24h)-20(28 days)	0.21

Despite the low compressive strengths measured (ranged between 0.10-0.48 MPa), a statistical analysis of the results was developed. Figure 3 plotted the mean of means as a function of the parameters studied; the optimum level for each factor is defined by the highest mean of means. The set of optimal conditions at 28 days was: 10 wt.% of CAC, 12 wt.% Na₂O, SiO₂/Na₂O ratio of 0 (pure NaOH solution) and curing at 40

°C for 28 days. The predicted 28 day-compressive strength was of 0.585 MPa and a confirmation experiment was conducted, and the paste registered 0.65 MPa.

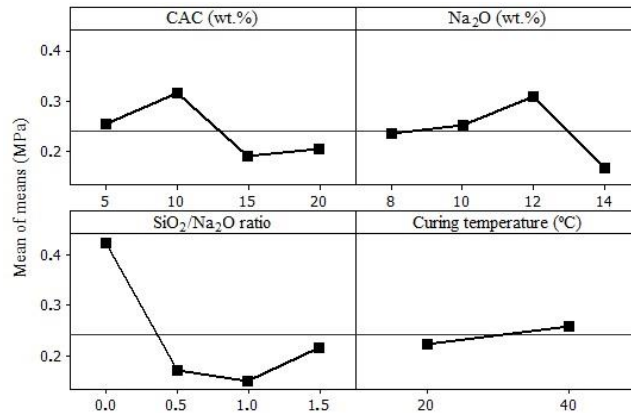


Figure 3. Effect of levels of each factor.

The analysis of variance (ANOVA) allowed the calculation of the weighed contribution of each factor on the compressive strength; the computed results are given in Table 5. The results showed that the SiO₂/Na₂O ratio was the most important factor with a contribution of 53.30 %, followed by 22.93% of contribution due to error, 11.62% due to wt.% Na₂O, 10.76% due to wt.% of CAC, with the least contribution of 1.38% for the curing temperature.

Table 5. ANOVA of compressive strength, contribution percentage of each factor.

Factors	Degrees of freedom	Sum of squares	% Contribution
CAC (wt.%)	3	0.03827	10.76
Na ₂ O (wt.%)	3	0.04132	11.62
SiO ₂ /Na ₂ O ratio	3	0.18953	53.30
Curing temperature (°C)	1	0.00490	1.38
Error	5	0.08155	22.93
Total	15	0.35558	100

Although the curing temperature was the factor with least contribution % on the compressive strength, some pastes were selected to be hardened at 100 or 200 °C for 2 h and then cured at 20 °C until 28 days. The selected formulations were described above in Table 2 and the 28 day-compressive strength is showed in Table 6. As can be seen from Table 6, the increase in the curing temperature from 100 to 200 °C caused a decrease in the compressive strength from 11 to 5.60, 20 to 5.10, and 8 to 7.70 MPa for pastes 95-10-0.5, 85-14-0.5, and 90-14-1, respectively. Conversely, paste 90-10-0 showed an increase almost twice from 6.13 to 11.43 MPa when increased the curing temperature from 100 to 200 °C. Overall, the paste 85-14-0.5 showed the highest 28-days compressive strength of 20 MPa when was hardened at 100 °C for 2 h. This highest 28 days-compressive strength of 20 MPa could be associated with the use of the highest content of CAC of 15 wt.% in this formulation, and the possible reaction of CaO and Al₂O₃ from CAC with SiO₂ from SCBA in an aqueous solution. C. Tippayasam and co-workers (Tippayasam et al., 2014) reported the use of 100 wt.% SCBA as a precursor for the production of AAC, obtaining 91 days-compressive strength of ~6MPa. However, when binary systems such as metakaolin/SCBA were used, higher 91 days-compressive strengths of ~17 MPa were achieved.

Although during hardened at 100 or 200 °C, all the specimens were covered with plastic films, the decrease in the compressive strength could be related to the loss of water needed for the formation of reaction products, nevertheless, further work is currently underway to identify the origin of this decrease.

Overall, our results stress the feasibility to use higher amounts of industrial waste as SCBA to obtain cementitious materials with compressive strength ranged from 5-20 MPa, close to the reported in the literature for metakaolin/SCBA composites (Tippayasam et al., 2014).

Table 6. 28 day-compressive strength of selected formulations.

Formulation	28 days-compressive strength (MPa)	
	100 °C	200 °C
95-10-0.5	11.00	5.60
90-10-0	6.13	11.43
90-14-1	8.00	7.70
85-14-0.5	20.00	5.10

3.3. Reaction products of SCBA-CAC composites

Figure 4 shows the XRD pattern for selected paste 95-10-0.5 cured at 100 and 200 °C. For comparison, it was introduced the XRD pattern of SCBA as raw material. SCBA presented an asymmetric halo between 15-33 °2θ, characteristic of amorphous materials, and this halo continued present in paste 95-10-0.5 activated at 100 and 200 °C, with a slight decrease in the intensity. In both cases, the albite and anorthite crystalline phases of the raw material continued present but no new phases from the hydration of CAC were observed, probably due to the low content of this precursor.

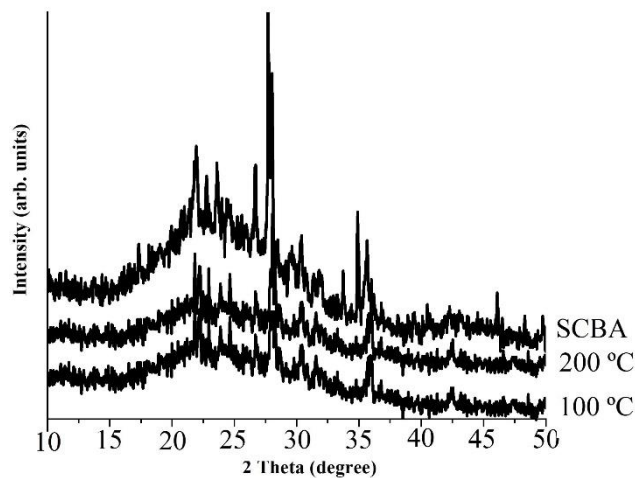


Figure 4. XRD pattern of selected paste 95-10-0.5 cured at 100 and 200 °C.

Figure 5 shows the XRD pattern for selected paste 85-14-0.5 cured at 100 and 200 °C. For comparing, the XRD pattern of SCBA as raw material was introduced. Again, the halo between 15-33 °2θ continued present in paste 85-14-0.5 activated at 100 and 200 °C, with a slight decrease in the intensity, however, for activation at 100 °C (paste with the highest 28 days-compressive strength of 20 MPa) the halo was displaced at higher values between 18-39 °2θ. It has been reported for metakaolin/FA composites (Arellano Aguilar et al., 2010; Criado et al., 2007) that in some cases the amorphous halo appears initially at 20-30 °2θ and after alkaline activation, the halo shifts towards values of 25-35 °2θ; said displacement suggests the formation of reaction products with an amorphous structure different from the precursor material. The albite and anorthite crystalline phases of the raw material are still present and the hydrated

CAC phases were not observed, despite the high wt.% of CAC used in this formulation. Similar results (not presented in this work) were observed for pastes 90-10-0 and 90-14-1 cured at 100 and 200 °C.

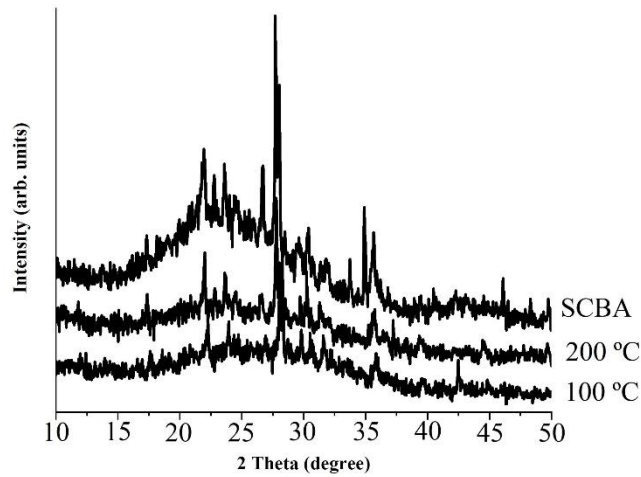


Figure 5. XRD pattern of selected paste 85-14-0.5 cured at 100 and 200 °C.

3.4. Microstructure of SCBA-CAC composites

Figure 6 presents the microstructure of selected paste 85-14-0.5 cured at 100 °C, with the highest 28-days compressive strength of 20 MPa. At low magnification (left), it can be seen an unreacted SCBA particle of around 50 μm in size, surrounded by a matrix of reaction products and some partially reacted particles. At higher magnification (right), this matrix of reaction products seems to be dense and the EDS analysis indicates that is probably formed by C-S-H, N-A-S-H, C-A-S-H, silica gel, or a combination of the four intimately mixed reaction products.

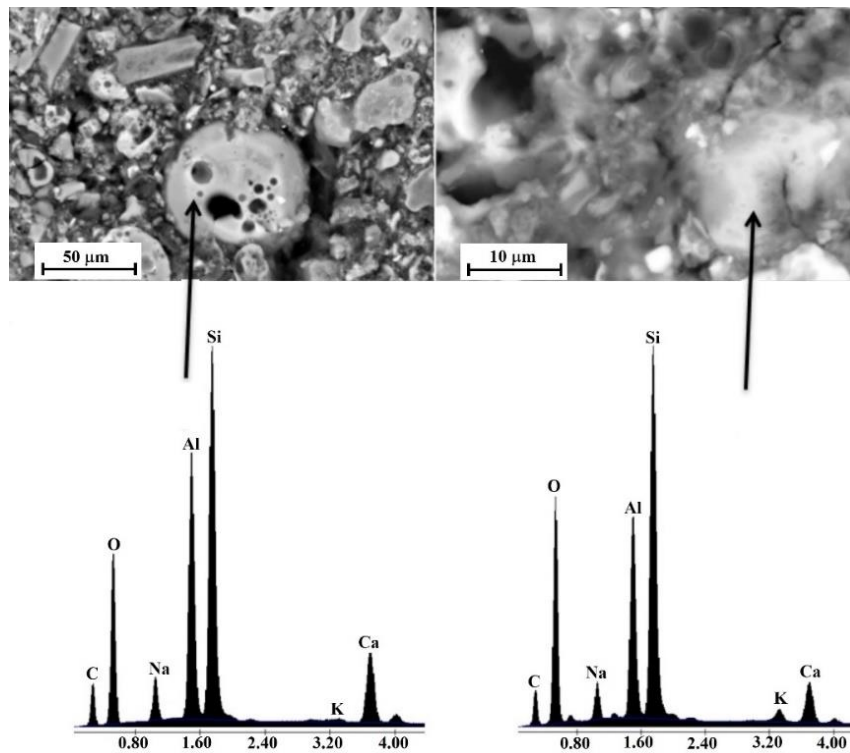


Figure 6. Microstructure of selected paste 85-14-0.5 cured at 100 °C.

Finally, Figure 7 shows the microstructure of selected paste 90-10-0 cured at 200 °C.

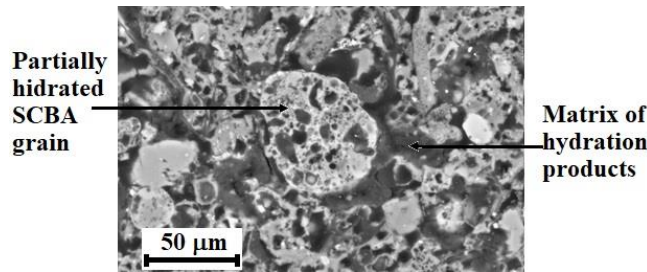


Figure 7. Microstructure of selected paste 90-10-0 cured at 200 °C.

The selected paste 90-10-0 showed a dense microstructure, with many SCBA grains partially reacted dispersed throughout. The SCBA grains did not show rims of hydration products, indicating that the SCBA reacted mainly by dissolution–precipitation mechanism. On the other hand, no CAC grains appeared. The hydration of CAC produces Ca^{2+} and Al^{3+} , which can be consumed by the SCBA to produce C-A-S-H gel that should contribute to the strength.

4. CONCLUSIONS

Pastes of high content of sugarcane bagasse ash were manufactured with replacements of 5-20 wt.% of calcium aluminate cement and activated with alkaline solutions of 8-14 wt.% of sodium silicate, varying the silica modulus between 0-1.5. The pastes were cured at 20 or 40 °C and showed poor mechanical performance, however, when selected pastes were cured at 100 or 200 °C for 2 h, reached compressive strengths between 5-20 MPa, which was attributed to the formation of a dense matrix of amorphous reaction products. In general, higher strengths were achieved when activating the pastes at 100 °C rather than 200 °C. Our results stress the feasibility to use industrial waste material such as sugarcane bagasse ash to obtain cementitious composites with compressive strengths between 5-20 MPa, nevertheless, further work is currently underway to identify the effect of variables on the compressive strength of composites.

5. ACKNOWLEDGMENTS

The authors would like to thank the National University of Engineering (UNI) of Nicaragua, Monte Rosa sugar mill of Nicaragua, and Center for Research and Advanced Studies of México for the support given to Zugania Zelmira Zúniga García to carry out this research.

REFERENCES

- Ali, M. B., Saidur, R., & Hossain, M. S. (2011). A review on emission analysis in cement industries. In *Renewable and Sustainable Energy Reviews*. <https://doi.org/10.1016/j.rser.2011.02.014>
- Arellano Aguilar, R., Burciaga Díaz, O., & Escalante García, J. I. (2010). Lightweight concretes of activated metakaolin-fly ash binders, with blast furnace slag aggregates. *Construction and Building Materials*. <https://doi.org/10.1016/j.conbuildmat.2009.12.024>
- Bahurudeen, A., & Santhanam, M. (2015). Influence of different processing methods on the pozzolanic performance of sugarcane bagasse ash. *Cement and Concrete Composites*. <https://doi.org/10.1016/j.cemconcomp.2014.11.002>
- Castaldelli, V. N., Moraes, J. C. B., Akasaki, J. L., Melges, J. L. P., Monzó, J., Borrachero, M. V., Soriano, L., Payá, J., & Tashima, M. M. (2016). Study of the binary system fly ash/sugarcane bagasse ash (FA/SCBA) in $\text{SiO}_2/\text{K}_2\text{O}$

alkali-activated binders. *Fuel*. <https://doi.org/10.1016/j.fuel.2016.02.020>

Castaldelli, Vinícius N., Akasaki, J. L., Melges, J. L. P., Tashima, M. M., Soriano, L., Borrachero, M. V., Monzó, J., & Payá, J. (2013). Use of slag/sugar cane bagasse ash (SCBA) blends in the production of alkali-activated materials. *Materials*. <https://doi.org/10.3390/ma6083108>

Cordeiro, G. C., Toledo Filho, R. D., Tavares, L. M., & Fairbairn, E. de M. R. (2009). Ultrafine grinding of sugar cane bagasse ash for application as pozzolanic admixture in concrete. *Cement and Concrete Research*. <https://doi.org/10.1016/j.cemconres.2008.11.005>

Criado, M., Fernández-Jiménez, A., de la Torre, A. G., Aranda, M. A. G., & Palomo, A. (2007). An XRD study of the effect of the SiO₂/Na₂O ratio on the alkali activation of fly ash. In *Cement and Concrete Research*. <https://doi.org/10.1016/j.cemconres.2007.01.013>

De Soares, M. M. N. S., Garcia, D. C. S., Figueiredo, R. B., Aguilar, M. T. P., & Cetlin, P. R. (2016). Comparing the pozzolanic behavior of sugar cane bagasse ash to amorphous and crystalline SiO₂. *Cement and Concrete Composites*. <https://doi.org/10.1016/j.cemconcomp.2016.04.005>

Escalante García, J. I. (2002). Materiales alternativos al cemento Pórtland. *Avance y Perspectiva*.

Menchaca-Ballinas, L. E., & Escalante-Garcia, J. I. (2019). Low CO₂ emission cements of waste glass activated by CaO and NaOH. *Journal of Cleaner Production*. <https://doi.org/10.1016/j.jclepro.2019.117992>

Morales, E. V., Villar-Cociña, E., Frías, M., Santos, S. F., & Savastano, H. (2009). Effects of calcining conditions on the microstructure of sugar cane waste ashes (SCWA): Influence in the pozzolanic activation. *Cement and Concrete Composites*. <https://doi.org/10.1016/j.cemconcomp.2008.10.004>

Payá, J., Monzó, J., Borrachero, M. V., Soriano, L., Akasaki, J. L., & Tashima, M. M. (2017). New inorganic binders containing ashes from agricultural wastes. In *Sustainable and Nonconventional Construction Materials using Inorganic Bonded Fiber Composites*. <https://doi.org/10.1016/B978-0-08-102001-2.00006-1>

Pour-Ghaz, M. (2013). Sustainable infrastructure materials: Challenges and opportunities. *International Journal of Applied Ceramic Technology*. <https://doi.org/10.1111/ijac.12083>

Tchakouté, Hervé K., Rüscher, C. H., Kong, S., Kamseu, E., & Leonelli, C. (2016). Geopolymer binders from metakaolin using sodium waterglass from waste glass and rice husk ash as alternative activators: A comparative study. *Construction and Building Materials*. <https://doi.org/10.1016/j.conbuildmat.2016.03.184>

Tchakouté, Hervé Kouamo, Rüscher, C. H., Hinsch, M., Djobo, J. N. Y., Kamseu, E., & Leonelli, C. (2017). Utilization of sodium waterglass from sugar cane bagasse ash as a new alternative hardener for producing metakaolin-based geopolymer cement. *Chemie Der Erde*. <https://doi.org/10.1016/j.chemer.2017.04.003>

Tippayasam, C., Keawpapasson, P., Thavorniti, P., Panyathanmaporn, T., Leonelli, C., & Chaysuwan, D. (2014). Effect of Thai Kaolin on properties of agricultural ash blended geopolymers. *Construction and Building Materials*. <https://doi.org/10.1016/j.conbuildmat.2013.11.079>

Turner, L. K., & Collins, F. G. (2013). Carbon dioxide equivalent (CO₂-e) emissions: A comparison between geopolymer and OPC cement concrete. *Construction and Building Materials*. <https://doi.org/10.1016/j.conbuildmat.2013.01.023>

Vafaei, M., & Allahverdi, A. (2017). High strength geopolymer binder based on waste-glass powder. *Advanced Powder Technology*. <https://doi.org/10.1016/j.apt.2016.09.034>

Xu, Q., Ji, T., Gao, S. J., Yang, Z., & Wu, N. (2018). Characteristics and applications of sugar cane bagasse ash waste in cementitious materials. In *Materials*. <https://doi.org/10.3390/ma12010039>